Archives of Biochemistry and Biophysics 591 (2016) 76–86

Contents lists available at ScienceDirect

Archives of Biochemistry and Biophysics

journal homepage: www.elsevier.com/locate/yabbi

Transbilayer asymmetry and sphingomyelin composition modulate the preferential membrane partitioning of the nicotinic acetylcholine receptor in Lo domains

Vanesa L. Perillo [a, b, 1], Daniel A. Peñalva [a, b], Alejandro J. Vitale [b, c], Francisco J. Barrantes [d], Silvia S. Antollini [a, b, *]

[a] Instituto de Investigaciones Bioquímicas de Bahía Blanca (CONICET-UNS), Camino La Carringanda Km 7, 8000 Bahía Blanca, Buenos Aires, Argentina
[b] Universidad Nacional del Sur, Av. Alem 1253, 8000 Bahía Blanca, Buenos Aires, Argentina
[c] Instituto Argentino de Oceanografía (CONICET-UNS), Camino La Carringanda Km 7, 8000 Bahía Blanca, Buenos Aires, Argentina
[d] Laboratory of Molecular Neurobiology, BIOMED UCA-CONICET, Av Moreau de Justo 1300, 1107 Buenos Aires, Argentina

ARTICLE INFO

Article history:
Received 28 September 2015
Received in revised form
2 December 2015
Accepted 10 December 2015
Available online 15 December 2015

Keywords:
Nicotinic acetylcholine receptors
Transbilayer asymmetry
Lipid raft
Fluorescence
Sphingolipids
Liposomes

ABSTRACT

We have previously shown that the intact nicotinic acetylcholine receptor (AChR) lacks preference for Lo domains when reconstituted in a sphingomyelin (SM), cholesterol (Chol) and POPC (1:1:1) model system (Bermúdez V, Antollini SS, Fernández-Nievas GA, Aveldaño MI, Barrantes FJ. J. Lipid Res. 2010; 51: 2629–2641). Here, we have furthered our studies by characterizing the influence of different lipid host compositions on the distribution of purified AChR reconstituted in two model systems (POPC:Chol, 1:1 and POPC:Chol:SM, 1:1:1), involving a) different SM species (porcine brain SM (bSM), 16:0-SM, 18:0-SM or 24:1-SM); or b) induced transbilayer asymmetry, resulting from enrichment in bSM in the external hemilayer. AChR distribution was evaluated by fluorescence resonance energy transfer efficiency between the AChR intrinsic fluorescence and Laurdan or dehydroergosterol fluorescence, and by analyzing the distribution of AChR in detergent-resistant and detergent-soluble fractions (1% Triton X-100, 4 °C). bSM-induced transbilayer asymmetry or the presence of 16:0-SM and/or 18:0-SM (unlike bSM or 24:1-SM) resulted in the preferential partitioning of AChR in Lo domains, suggesting that the localization of AChR in ordered domains strongly depends on the characteristics of the host lipid membrane, and in particular on the sphingolipid composition and transbilayer asymmetry.

1. Introduction

The nicotinic acetylcholine receptor (AChR) is an integral membrane protein, belonging to the Cys-loop superfamily of ligand-gated ion-channels [1]. It has five subunits ($(\alpha_1)_2\beta\delta\gamma$) in embryonic muscle of vertebrates [2], each composed of a large N-terminal extracellular domain, four transmembrane segments (M1-M4), a small cytoplasmic domain between M3 and M4, and a short C-terminal extracellular domain [3]. The transmembrane region of the AChR exhibits extensive contacts with the surrounding lipids through structural motifs remarkably conserved along phylogenetic evolution [4,5].

AChR is one of the key players of the post-synaptic components in neuromuscular junction, localizing in high-density clusters at the top of folds in the muscle cell membrane [6,7]. The clustering mechanism begins with the activation of the muscle-specific receptor tyrosine kinase (MuSK) by neural agrin, triggering an intracellular signaling cascade that ends with the binding of the peripheral protein rapsyn to AChR and thus modulating both AChR clustering and its immobilization to the cytoskeleton [8]. Several lines of evidence suggest that these clusters localize in heterogeneous membrane domains highly enriched in cholesterol (Chol) and sphingolipids, and that Chol has a high importance in the biogenesis and stability of AChR clustering [9–16].

Domains rich in Chol and sphingolipids are commonly known as raft [17]. One hypothesis of raft domains, named *the condensed complexes and lipid shell model* [18], is that they are chemical complexes of Chol and sphingolipids formed in a reversible reaction where the equilibrium thermal fluctuation of this reaction may

* Corresponding author.
E-mail address: silviant@criba.edu.ar (S.S. Antollini).
[1] Current address: Department of Plant and Soil Science, University of Vermont, Burlington, Vermont, United States of America.

http://dx.doi.org/10.1016/j.abb.2015.12.003
0003-9861/

give rise to transient and small Lo domains (i.e., liquid rich in condensed complexes) (reviewed in [18]). In the case of transmembrane proteins surrounded by specific lipids, these domains could help create specific lipid environments by an effect of wetting and that, at high protein concentration, these selected microenvironments can percolate and generate lipid aggregation at large scales [18]. A more recent hypothesis postulates that actin filaments also contribute to this mayor domain aggregation, which affects both the local membrane composition and shape, driving the membrane out of equilibrium [19]. It gives equal importance to the interactions between membrane entities and the ones between membrane molecules and cortical actin. This last hypothesis is named *the active composite cell surface model* and explains the nanoclustering process by actomyosin interactions [18].

But how does the AChR localize in raft domains in the first place? Is it already there or does neural agrin signaling force the AChR to move into these more rigid and thicker domains [20]? Some studies suggest that AChR localizes in raft domains independently of neural agrin stimulation [21], whereas other studies suggest that AChR localizes in non-raft domains and moves into these domains after MuSK activation [9]. A synthetic peptide corresponding to the M4 transmembrane segment of the AChR γ subunit was found to exhibit a definite preference for localizing in the liquid-ordered (Lo) phase in a model lipid system [22]. In contrast, the whole AChR distributed both in Lo and liquid-disordered (Ld) domains upon reconstitution in SM:Chol:POPC (1:1:1) model membranes [23]. Thus, we hypothesized that although the M4 segment gives the AChR the potential to localize in raft domains, it still needs external signals that influence AChR partition profile [23].

Some transmembrane proteins are targeted to raft domains by the presence of specific amino acid sequences either in their intracellular [24], extracellular [25] or transmembrane [26] domains; other membrane proteins do so by lipid modifications such as palmitoylation [27] or myristoylation [28]. An additional hypothesis poses that the lipids that surround transmembrane proteins might have an effect on their location and lead them to localize in these more ordered domains [29]. In this work, we provide evidence supporting the latter hypothesis by showing that membrane sphingomyelin (SM) composition and/or lipid transbilayer asymmetry play a key role in AChR preference for raft domains.

2. Materials and methods

2.1. Materials

Torpedo californica specimens were obtained from Aquatic Research Consultants (San Pedro, CA) and maintained at −70 °C until use. Laurdan, dehydroergosterol (DHE), 1,6-diphenyl-1,3,5-hexatriene (DPH) and 1-(4-Trimethylammoniumphenyl)-6-Phenyl-1,3,5-Hexatriene p-Toluenesulfonate (TMA-DPH) were purchased from Molecular Probes (Eugene, OR). Affi-Gel 10 Gel and dithiothreitol were obtained from Bio-Rad. Synthetic lipids were from Avanti Polar Lipids, Inc. (Birmingham, AL). [^{125}I]alpha-Bungarotoxin (α-BTX) was purchased from New England Nuclear (Boston, Mass., USA). All other drugs were obtained from Sigma–Aldrich.

2.2. Methods

2.2.1. 16:0 and 18:0 sphingomyelin purification

Lipids were extracted from the yolk of a 10-min boiled egg (for N-(hexadecanoyl)-sphing-4-enine-1-phosphocholine (16:0-SM)) and from rat testes homogenate (for 16:0-SM and N-(octadecanoyl)-sphing-4-enine-1-phosphocholine (18:0-SM)) according to the procedure of Bligh and Dyer [30]. Rat testes were obtained from 10 Wistar rats aged 3–4 months, bred at the Instituto de Investigaciones Bioquímicas de Bahía Blanca (INIBIBB), weighing between 300 and 350 g. The animals were sacrificed by cervical dislocation after a brief exposure to CO_2 and used immediately. Testes were decapsulated and, after removing visible blood vessels, were rinsed in saline. Lipid extracts were prepared using mixtures of chloroform-methanol. All proceedings were carried out in strict accordance with the *National Institutes of Health Guide for the Care and Use of Laboratory Animals* (NHI) and were approved by the Institutional Committee for the Care of Laboratory Animals (CICUAE) from the Universidad Nacional del Sur (Argentina).

Lipids were then resolved into classes by thin layer chromatography (TLC) on silica gel H-plates, and spotted under UV light after spraying with dichlorofluorescein. TLC was performed using chloroform–methanol–amonium hydroxide (65:25:5, v/v/v) as the developing solvent to separate SM from PC. The SM band was scraped and eluted, then the species present were checked by Gas Chromatography (GC) and purified by High Pressure Liquid Chromatography (HPLC) according to Peñalva et al. [31]. Samples were kept at −20 °C until use.

2.2.2. Affinity column preparation and AChR purification

The AChR was purified from *T. californica* electric tissue. Briefly, electric tissue was chopped into small pieces, homogenized using a Virtis homogenizer under controlled conditions, and submitted to a centrifugation step of 2 hs at 40,000 g and 4 °C, obtaining *T. californica* crude membranes. Those membranes were then solubilized in 1% sodium cholate (2 mg/ml protein concentration) for 45 min at 4 °C and then centrifuged at 74,000 g for 1 h to discard the insoluble material. The AChR was purified by affinity chromatography in the presence of synthetic lipids [32]. Briefly, the affinity column was prepared by coupling cystamine to Affi-Gel 10, reduction with dithiothreitol, and final modification with bromoacetylcholine bromide. The supernatant was applied to the affinity column. To facilitate complete exchange of endogenous for defined lipids, the column was then washed with a linear gradient of defined lipids, consisting of either POPC:SM:Chol (1:1:1), POPC:SM:Chol (0.35:1:0.87) or POPC:Chol (1:1), dissolved in dialysis buffer (100 mM NaCl, 0.1 mM phosphate, 0.1 mM EDTA, 0.02% NaN_3, pH 7.8) containing 1% cholate, from 1.3 to 3.2 mM and then to 0.13 mM lipid concentration [32]. The type of SM varied between bSM, 16:0-SM, 18:0-SM, and 24:1-SM. The AChR was then eluted from the column with a 0.13 mM lipid solution in 250 mM NaCl, 0.1 mM EDTA, 0.02% NaN_3, 5 mM phosphate, pH 7.8, with 0.5% cholate and 10 mM carbamylcholine (Carb). After elution from the column, the AChR was dialyzed against 1 L of dialysis buffer with five buffer changes (every 12 hs) at 4 °C. AChR purity was checked by SDS-PAGE, and protein concentration was determined by the method of Lowry [33]. The orientation of AChR in the membrane vesicles was determined as described by Hartig and Raftery [34] by comparing the total toxin binding sites in the presence of Triton X-100 and the right-side-out toxin binding sites in the absence of detergent as in previous work from our laboratory [35]. The samples were stored at −70 °C until use.

2.2.3. Lipid-only liposome preparation

0.6 mg of the desired lipid mixture were dried for 1 h under N_2. Subsequently, liposomes were resuspended in dialysis buffer at 45°C (0.5 mg/ml), vortexed for 1 min and sonicated for 30 min.

2.2.4. Induction of transbilayer asymmetry

To generate asymmetry in the model membrane, a lipid interchange with methyl-β-cyclodextrin (MβCD) in the outer leaflet was

made according to Cheng et al. [36]. Briefly multilamellar vesicles (MLVs) made of bSM were obtained (2 mM). 250 μL of MLVs were incubated against 47.5 μL of MβCD (195 mM), vortexing for 2 h at 55 °C, obtaining a mixture of MLVs and MLVs/MβCD. AChR-containing liposomes (250 μL, 0.5 mM total lipid) were mixed with an equal volume of the MLVs/MβCD-MLVs mixture, vortexing for 20 min at 37 °C. An initial centrifugation step at 49,000 g for 5 min at 4 °C removed the exceeding MLVs (pellet), followed by another centrifugation step at 100,400 g for 1 h and 4 °C, which removed the MβCD (supernatant). Asymmetric liposomes were resuspended in Buffer A (150 mM NaCl, 0.25 mM $MgCl_2$, and 20 mM HEPES buffer, pH 7.4) for fluorescence measurements or in 10 mM phosphate buffer for α-BTX binding experiments. Samples were used on the same day to avoid possible loss of asymmetry.

2.2.5. Scrambling and reconstitution of vesicles

Asymmetric liposomes were dried under N_2, dissolved with chloroform:methanol (2:1 v/v) and reconstituted at 55 °C with 980 μL of distilled water. These samples were subsequently used for fluorescence studies.

2.2.6. Giant unilamellar vesicle formation

50 μg of a lipid mix composed of POPC:Chol:SM (1:1:1) dissolved in organic solvent and the fluorescent probe (DiI) (<0.2%) were dried on an ITO slide from Vesicle Prep-Pro (Nanion, Munich, Germany). Quickly, 200 μL of 0.5 M sucrose was added and the chamber was sealed with a second ITO slide. Conditions for the run were as follows: 4.33 h, 1.3 V and 500 Hz at 45 °C. GUVs were observed in a Nikon E-600 fluorescence microscope (Nikon Instruments Inc., Melville, NY, E.E.U.U.) and the obtained images were analyzed with Image J software (National Institutes of Health, Bethesda, MD) [37].

2.2.7. Preparation of detergent-resistant and detergent-soluble membrane fractions

Either 60 μg of purified AChR reconstituted in liposomes or lipid-only liposomes (0.6 mg of total lipid) were treated with 1% Triton X-100 for 20 min at 4 °C. The samples were then separated into detergent resistant and detergent soluble membrane fractions (DRM and DSM, respectively) by centrifugation at 104,000 g for 4 hs at 4 °C in a TLA 100.4 rotor using a Beckman Optima TLX centrifuge. The supernatant (DSM) was removed, and the pellet (DRM) was resuspended in an equal volume of buffer (10 mM phosphate, pH 7).

2.2.8. Lipid characterization of the DSM and DRM fractions

In lipid-only liposomes, samples were treated as in Bermúdez et al. [23]. Briefly, Triton X-100 was eliminated from the DSM and DRM fractions by washing the samples with SM-2 Biobeads and the lipids of each fraction were afterward extracted [30], resolved into classes by TLC on commercial silica gel G-plates, and spotted under UV light after spraying with dichlorofluorescein. TLC was performed using chloroform-methanol-acetic acid-0.15 M NaCl (20:10:3.2:1, v/v/v/v) as the first developing solvent to separate SM from PC, followed by ether as the second one up to the top of the plate to separate Chol from the phospholipids. The spots corresponding to SM, PC and Chol were scraped off, and the lipid phosphorus and Chol content were determined by Rouser et al. [38] and cholesterol oxidase assay (Wiener Laboratories, Rosario, Argentina), respectively.

2.2.9. [^{125}I]α-BTX binding experiments

The presence of AChR in DRM and DSM fractions was determined by incubating samples with [^{125}I]α-BTX (40 nM) for 1 h at room temperature. At the end of the incubation period, each sample was poured into 2 × 2 cm DEAE paper strips pinned onto a Styrofoam base. Once the strips were dry, they were washed four times in 10 mM phosphate buffer (pH 7.4) containing 100 mM NaCl and 0.1% Triton X-100. Each strip was put into a tube and radioactivity was measured in a γ-counter with an efficiency of 80%. Non-specific binding was determined both by heating the samples at 100 °C for 5 min or by adding 1 mM carbamoylcholine before addition of [^{125}I]α-BTX.

2.2.10. Fluorescence measurements

Samples for fluorescence measurements consisted in 10–14 μg protein/ml of the reconstituted AChR liposomes suspended in buffer A, keeping the optical density below 0.1 to minimize light scattering. Fluorescent probes dissolved in organic solvents were added to the samples (the amount of organic solvent was kept below 0.2%), incubated for 45 min to allow equilibration, and then the emission spectra were collected. All fluorimetric measurements were performed in an SLM model 4800 fluorimeter (SLM Instruments, Urbana, IL) using a vertically polarized light beam from Hannovia 200-W mercury/xenon arc obtained with a Glan-Thompson polarizer (4-nm excitation and emission slits) and 1-ml quartz cuvettes. The temperature was set at 4 °C or at 42 °C with a thermostated circulating water bath (Haake, Darmstadt, Germany).

2.2.11. Förster resonance energy transfer (FRET) measurements

Samples were incubated either with Laurdan or DHE and fluorescence measurements were taken before and after the addition of probes (I_0 and I, respectively). The excitation and emission wavelengths were 290 and 330 nm, respectively. FRET efficiency (*E*) was calculated according to Förster theory [39] as follows:

$$E = 1 - \frac{I}{I_0} \tag{1}$$

AChR preferential partition profile was analyzed according to Bermúdez et al. [23]. Briefly, an *E*-value ratio between the fluorescent probes DHE and Laurdan ($E_{DHE}/E_{Laurdan}$) with the RAFT-like model (POPC:Chol:SM 1:1:1) was obtained. Due to overlapping differences between the absorption spectra of the probes and the emission spectra of the intrinsic fluorescence plus differences in their quantum yields, a correction ratio ($E_{DHE}/E_{Laurdan}$) was obtained using a DRM-like model (POPC:SM:Chol, 0.35:1:0.87). Since in the DRM-like model both pairs of donor-acceptor have the same probability of FRET, this ratio should be close to unity. Any difference to the unity reflects the above mentioned differences, and thus this correction ratio was therefore used as a correction factor for the RAFT-like model. In this system, when donor molecules (AChR) localize in both types of domains, E_{DHE} should be near half the $E_{Laurdan}$ value, giving an $E_{DHE}/E_{Laurdan}$ value close to 0.5. If the donor molecule preference is for liquid disordered domains, the ratio should be close to zero. Lastly, if donor molecules locate at liquid ordered domains, E_{DHE} should be significantly larger than $E_{Laurdan}$, giving a ratio greater than 1.

2.2.12. Generalized polarization

Laurdan experiments were carried out as in Antollini and Barrantes [40] using a final probe concentration of 0.6 μM. Generalized polarization (GP) was calculated as follows [41]:

$$GP = \frac{I_{434} - I_{490}}{I_{434} + I_{490}} \tag{2}$$

where I_{434} and I_{490} are the emission intensities at the characteristic wavelengths of the gel and liquid-crystalline phases, respectively.

Excitation wavelength was 360 nm.

2.2.13. Fluorescence anisotropy

Anisotropy (r) measurements of DPH or TMA-DPH (0.6 μM final concentration) were made as described previously [40,42]. The excitation and emission wavelengths used were 365 and 425 nm, respectively. Fluorescence anisotropy measurements were done in the T format with Schott KV418 filters in the emission channels and corrected for optical inaccuracies and background signals. The anisotropy value, r, was obtained according to the following equation [43]:

$$r = \frac{(I_v/I_h)_v - (I_v/I_h)_h}{(I_v/I_h)_v + (I_v/I_h)_h} \quad (3)$$

where $(I_v/I_h)_v$ and $(I_v/I_h)_h$ are the ratios of the emitted vertically or horizontally polarized light to the excited vertically or horizontally polarized light, respectively.

2.2.14. Data analysis

Intergroup comparisons were carried out using one-way ANOVA test with the values representing the average ± SD of the total number of samples indicated in each figure legend. *, statistically significant differences ($p < 0.05$). **, *** statistically very significant differences ($p < 0.01$ and $p < 0.001$, respectively).

3. Results

3.1. Sphingomyelin-dependent AChR preferential partitioning in Lo domains

Different SM species result in the formation of Lo domains of different sizes [44]. To test whether this is the case, giant unilamellar vesicles (GUVs) of defined lipid composition (POPC:Chol:SM 1:1:1) were prepared with N-(hexadecanoyl)-sphing-4-enine-1-phosphocholine (16:0-SM), N-(octadecanoyl)-sphing-4-enine-1-phosphocholine (18:0-SM), N-(15Z-tetracosenoyl)-sphing-4-enine-1-phosphocholine (24:1-SM) and porcine brain sphingomyelin (bSM, mainly composed of 18:0-SM (50%) and 24:1-SM (21%)). As shown in Fig. 1, the size of the Lo domains was assessed by fluorescence microscopy. Vesicles composed of POPC:Chol:bSM (1:1:1) contain Lo domains [45]; however these domains were not large enough to be visible by conventional optical microscopy (Fig. 1a); a similar result was obtained with 24:1-SM (Fig. 1b). In contrast, 16:0-SM (Fig. 1c) did produce large visible domains, and 18:0-SM (Fig. 1d) produced much smaller, barely visible domains beyond the resolution of our optical setup.

In a second series of experiments we studied the influence of the different SM species on membrane order. AChR-containing large unilamellar liposomes (LUVs) were incubated with the fluorescent probe Laurdan and the GP value was determined for each reconstituted system. Fig. 2 shows that 16:0-SM and 18:0-SM at 4 °C had a significant higher membrane order than bSM and 24:1-SM, corroborating the prevalence of Lo domains for the two former SM species.

In a third series of experiments we analyzed the influence of SMs on the composition of the DRM/DSM fractions prepared from detergent extracts. Pure lipid LUVs having a composition of POPC:Chol:SM (1:1:1) were prepared, again varying the SM species. The LUVs were subsequently treated with 1% Triton X-100 and the lipid content of DRM and DSM was measured (Fig. 3). In the presence of bSM, 24:1-SM and 18:0-SM there was a small prevalence of the DSM fraction, whereas 16:0-SM induced an increase in the DRM fraction (Fig. 3a). When the individual lipid distribution was analyzed (Fig. 3b), the increase of 16:0-SM in the DRM fraction was clearly apparent, without a concomitant increment of either POPC or Chol. According to the phase diagram of de Almeida et al. [45], enrichment in SM without changing the proportion of the other two lipids induces a more rigid phase. Thus, 16:0-SM, and also 18:0-SM to a lesser extent, induced biophysically different DRM fractions.

We next studied the partitioning profile of the AChR in these fractions using two different methodologies. First, we treated the different model membranes with 1% Triton X-100 at 4 °C and prepared DRM and DSM. Each fraction was then labeled with [^{125}I] α-BTX and the distribution of toxin-labeled receptor measured in each fraction (Fig. 4a). [^{125}I]α-BTX was assumed to have the same affinity for the AChR in each fraction, as it has been done in other works [9,10]. The presence of 16:0-SM and of 18:0-SM resulted in a preferential partitioning of AChR in DRM fractions, whereas in the presence of 24:1-SM the AChR failed to show preference for a given fraction. The AChR exhibited no preference for DRM in LUVs containing bSM.

Detergent solubilization techniques are still controversial, since DRM fractions cannot be unequivocally correlated with Lo or "raft" domains [46]. We therefore performed an additional series of Förster resonance energy transfer (FRET) experiments, which did not involve detergent solubilization or membrane fractionation. FRET efficiencies (E) were calculated using the AChR intrinsic fluorescence as the donor and two different fluorescent probes as acceptors. One of the acceptor fluorescent probes was dehydroergosterol (DHE), an analog of Chol, which shows a preference for Lo domains [47–49]. The second fluorescent probe was Laurdan, which distributes homogeneously in the membrane [50,51]. The ratio of the two efficiencies ($E_{DHE}/E_{Laurdan}$) allowed us to determine the AChR partitioning in the different model membranes, as in Bermúdez et al. [23]. (see Methodology Section for details). Fig. 4b shows that all SMs behaved as in the membrane solubilization study: the presence of bSM or 24:1-SM in LUVs had no effect on the preference of AChR for either domain, whereas the presence of 18:0-SM or 16:0-SM led to a preferential localization of AChR in Lo domains (see Fig. 4b). Control experiments were performed at 42 °C, a temperature at which the membrane becomes completely fluid, with no coexistence of domains; thus, both probes should be homogeneously distributed across the membrane, having high probability of interaction with all the AChR molecules. Under these conditions, the $E_{DHE}/E_{Laurdan}$ ratio had values close to 1 (Fig. 4c), significantly different from those found at 4 °C (Fig. 4b).

3.2. Induction of transbilayer asymmetry and membrane order

Due to the methodological techniques, model membranes generally lack asymmetry. This is a drawback, since one fails to reproduce the transbilayer asymmetry of native membranes with raft domains purported to lie in the outer leaflet [20,52]. Previous studies from our group determined that AChR lacks preference for Lo domains when reconstituted in a *symmetrical* model system composed of the ternary mixture POPC:Chol:SM (1:1:1) [23]. Here we tested whether transbilayer asymmetry affected the ability of the AChR to localize in Lo domains. To this aim, we induced transbilayer asymmetry by addition of bSM to the external hemilayer [36] of AChR-containing symmetric LUVs. Briefly, symmetrical LUVs were exposed to a concentrated solution of MβCD loaded with bSM. Only the outer hemilayer of the LUVs exchanges lipids with the bSM-MβCD complexes, generating an asymmetric bSM-rich external hemilayer. Two model systems were prepared: the same as in Bermúdez et al. (POPC:Chol:SM, 1:1:1) [23] and another one lacking SM (POPC:Chol, 1:1), which acted as a control for the SM enrichment procedure. Based on the phase diagram of de Almeida et al. [45], the ternary lipid mixture allows the coexistence of Lo and

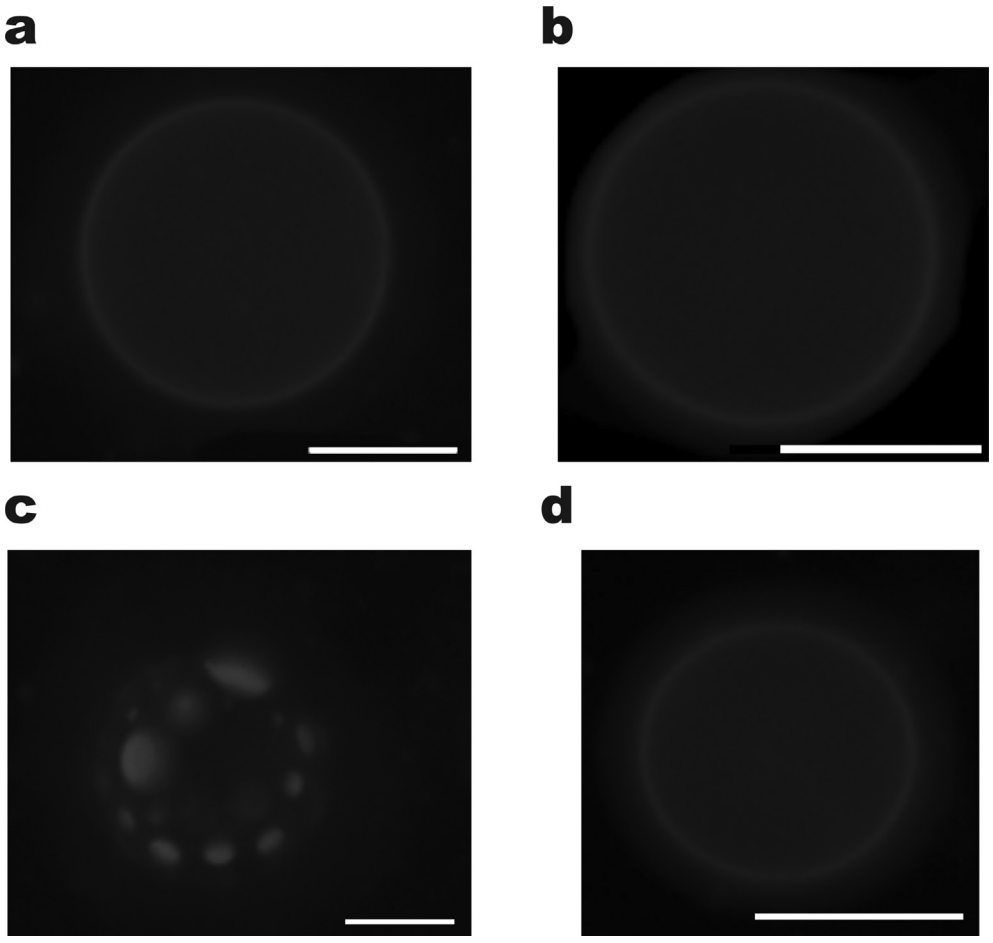

Fig. 1. Fluorescence microscopy of giant unilamellar vesicles (GUVs) containing different SM species. GUVS were made of POPC:SM:Chol (1:1:1) with the different SM species studied: (a) bSM, (b) 24:1-SM, (c) 16:0-SM and (d) 18:0-SM. GUVs were imaged at room temperature with the fluorescent probe DiIC12. Lo and Ld domains are shown in black and gray, respectively. Bars represent 10 μm.

Ld domains, whereas the binary lipid mixture maintains a Lo membrane organization [45].

Ideally a symmetric vesicle should not maintain the same membrane order as an asymmetric vesicle with the same lipid composition [36]. Therefore, to verify the success of the asymmetry induction protocol, an aliquot of the asymmetric samples was dried, their lipids scrambled with chloroform:methanol (2:1) and then reconstituted into symmetric vesicles of the exact same lipid composition. The membrane order of the asymmetric and the scrambled sample was then measured using the fluorescence anisotropy of two fluorescent probes. These probes localize at different levels inside the membrane, thus allowing the comparison of membrane order at different depths. DPH, an apolar molecule, inserts deep inside the hydrophobic core of the membrane, whereas TMA-DPH, which has a positively charged amino group, anchors near the surface of the external hemilayer [53]. Scrambled vesicles showed lower values of both DPH and TMA-DPH anisotropy than the corresponding values for asymmetric vesicles (Fig. 5), confirming the existence of different lipid arrangements in both vesicles despite having the same lipid composition. Membrane order in asymmetric vesicles remained the same after 20 h, confirming the maintenance of the asymmetry. Furthermore, anisotropy values of symmetric vesicles prepared with higher content of bSM (POPC:Chol:bSM 1:1:2 or 1:1:3) were lower than those of asymmetric vesicles. This result suggests that the asymmetric vesicles have a high membrane order in the outer membrane hemilayer.

Next, we compared the membrane order of symmetrical vesicles (prior to loading the SM) with the corresponding asymmetrical vesicles. The symmetrical vesicles of the two model systems studied showed similar fluorescence anisotropy values for both DPH and TMA-DPH (Fig. 6). After adding SM, both model systems showed an increment of the DPH anisotropy (Fig. 6a); and a diminution of the TMA-DPH anisotropy (Fig. 6b). To understand this discrepancy, and considering that TMA-DPH locates at the outer leaflet, we first checked if the treatment with SM-MβCD removed Chol from the external hemilayer and hence decreased its membrane order. We analyzed the lipid content of the supernatant obtained after the centrifugation step realized to separate the MβCD from the obtained asymmetrical samples. This supernatant must contain MβCD, the excess of bSM MLVs and lipids potentially extracted during the procedure. A TLC plate showed that very little Chol was extracted during the procedure (Fig. 7). This was not surprising because it is well documented that, in ternary lipids with ordered domains, empty MβCD has a slow depletion rate of Chol from the membrane, in some cases with no extraction of Chol at all [54]. This was explained considering the high Chol affinity for SM and that SM orientation hides Chol from MβCD in an umbrella-like manner [54]. If we consider that in this case the MβCD was not empty but loaded with SM, which enriched with this lipid the outer hemilayer, the possibility of Chol extraction was probably even lower, as it can be appreciated in Fig. 7. This result, together with the fact that cholesterol has a rapid flip-flop between hemilayers [55] and hence a loss of Chol from the outlet hemilayer should

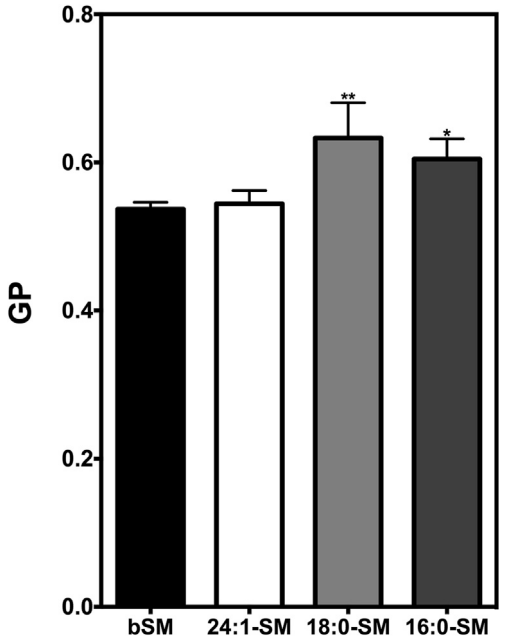

Fig. 2. Generalized Polarization (GP) of Laurdan in POPC:Chol:SM (1:1:1) membranes with purified AChR containing different SM species. Laurdan spectra were obtained with an excitation wavelength of 360 nm at 4 °C. Each column corresponds to the average ± SD of at least three different experiments. The comparison was performed with respect to liposomes containing bSM (control condition).

induce a decrease of the whole membrane order, discards that a loss of Chol from the sample was behind the lower membrane order measured by TMA-DPH. An alternative explanation is that TMA-DPH is excluded from the new external domains, richer in SM and hence with an increased membrane order according to de Almeida et al. [45]. To test this possibility, we used a third fluorescent probe, Laurdan, which locates superficially in both hemilayers because of a rapid flip-flop between them. Fig. 6c shows that the values of GP increased after SM treatment, indicating that the whole membrane augmented its order by addition of SM to the external hemilayer. This last experiment supports the idea that TMA-DPH is not able to sense the newly formed domains. In accordance with this explanation, recently Lin and London [56] postulated that Lo domains of the outer leaflet of asymmetric GUVs obtained with a similar protocol are so tightly packed that NBD-DPPE partitions into them poorly, whereas the Lo domains of the inner leaflet may be less tightly packed as NBD-DPPE partitions into them more favorably. Thus, the variation in the biophysical properties of the samples by induction of transbilayer asymmetry should be explored only with the probes DPH and Laurdan. The reported increment in Laurdan GP and DPH anisotropy values must therefore arise mainly from the external hemilayer as the SM is a polar lipid with a very slow flip-flop between hemilayers [57].

An additional measurement was performed with DPH and TMA-DPH at 42 °C (Fig. S1), temperature at which these domains disrupt and all lipids adopt a disordered phase [45]. Considering this condition as null existence of domains, we calculated a value that expresses the variation of domains ($\Delta_{domains}$) at 4 °C between control condition (r_{cont}) and asymmetric condition (r_{as}), as follows:

$$\Delta_{domains} = \frac{r_{as4^\circ C} - r_{as42^\circ C}}{r_{cont4^\circ C} - r_{cont42^\circ C}} \quad (4)$$

The ratio obtained for POPC:SM:Chol (1:1:1) with DPH was 1.66, indicating that asymmetry caused an increment in the amount of *rigid domains* with respect to the control condition. The TMA-DPH value was 1.12, reinforcing that this probe does not sense the newly formed domains. When the same analysis was performed for POPC:Chol, the value for DPH was 1.95, indicating that the addition of a third lipid caused an effective domain formation. In contrast, with TMA-DPH, the value was 0.72, showing a clear preference of this probe for the induced disordered domains, which are not present in the control situation.

If the addition of SM induces an asymmetry in the bilayer together with an increment in the amount of *rigid* domains in the external hemilayer, what effect does this have on the location of AChR? To answer this, we used the same techniques as in the previous section: detergent-mediated membrane solubilization evaluated with [^{125}I]α-BTX binding and FRET studies. When samples composed of POPC:Chol:bSM (1:1:1) were enriched in bSM in their external hemilayer, the AChR was preferentially found in the DRM fraction (Fig. 8a) and in *rigid*-domains (Fig. 8b). In the case of POPC:Chol (1:1), the control sample showed already a preference for AChR location in DRM and Lo domains. The incorporation of the third lipid in the system, SM, which changes the compartmentalization of the membrane, does not change the AChR distribution, remaining mainly in DRM or *rigid*-domains. Finally, to check that the fluorescent probes were located as it was postulated and were not perturbed by the previous membrane treatments, we performed a similar experiment at 42 °C, condition with no coexistence of domains. As in Fig. 4c, the $E_{DHE}/E_{Laurdan}$ ratio calculated at 42 °C was different to the one calculated at 4 °C, getting in all cases a value close to 1 (see Fig. 8c).

4. Discussion

The present study is an attempt to understand possible factors contributing to the possible localization of the AChR in different membrane lipid domains. In a previous work from our laboratory, it was found that the intact AChR oligomer lacks preference for a given membrane domain when reconstituted in a sphingomyelin (SM), cholesterol (Chol) and POPC (1:1:1) model system [23], although a synthetic version of M4 transmembrane segment exhibits a natural tendency to partition in Lo domains [22,23]. Thus, the location of the AChR in a given domain must result from a necessary but not sufficient intrinsic propensity of the AChR protein to insert into these membrane regions plus additional extrinsic factors. Here we investigated some of the potential extrinsic factors that bear on lipid membrane properties. It is well known that natural membranes present both lateral and transbilayer asymmetry [58]. In addition, transmembrane proteins have affinity for certain membrane lipids, inducing a lipid rearrangement around their transmembrane domains [59]. Transmembrane bilayer asymmetry was explored in a previous work from our laboratory [60] in native membranes, but these factors were not assayed in our studies using symmetrical model systems [23].

Here we first focused on SM, which together with cholesterol (Chol), is a key component of Lo domains [17]. In native membranes, SM mostly contains sphingosine as the long-chain base and 16:0, 18:0 or 24:1 as the N-linked acyl chain [61]. The three species confer a high degree of order to the membrane albeit to different extents [62]. Jaikishan and Slotte [44] indicated that 16:0-SM has the best hydrophobic match with Chol. Here we studied whether the differences between SM species (as compared to bSM, which contains mostly 18:0 and 24:1) had an influence on the localization of the AChR in a given membrane domain. The four model systems studied here, differing only in the SM type (16:0-SM, 18:0-SM, 24:1-SM, bSM), exhibit coexistence of domains (DRM and DSM, Fig. 3). However, these domains differ in size. The model system that contained 16:0-SM was the one with the visibly larger Lo domains (Fig. 1 and Fig. 3). 18:0-SM induced this effect, albeit with lower

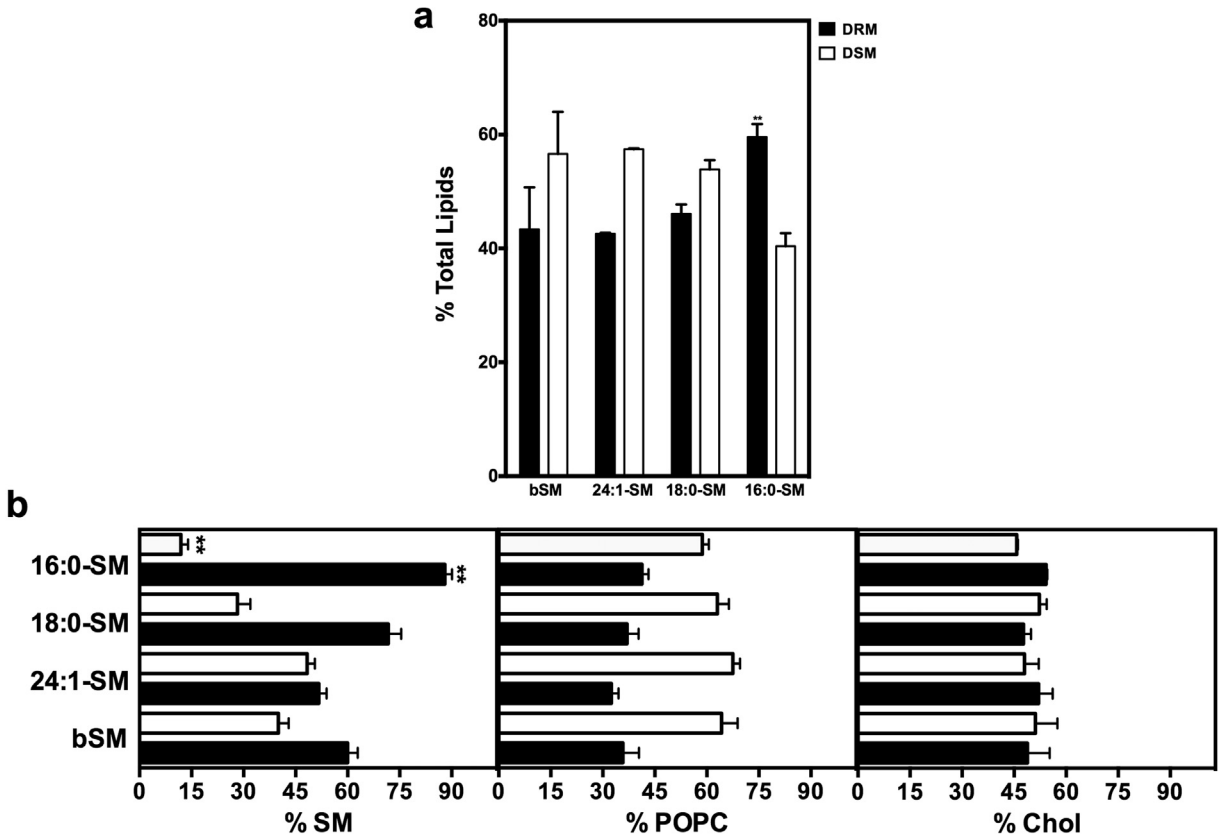

Fig. 3. Lipid characterization of DRM and DSM fractions obtained from POPC:Chol:SM (1:1:1) membranes with different SM species. (a) Total lipid comparison of each DRM and DSM fractions (black and white columns, respectively) as a function of the different SM studied. (b) Comparison of the lipid composition in the DRM (black bars) and DSM (white bars) fractions as a function of the different SM studied. Each column/bar corresponds to the average ± SD of at least three different experiments. The comparison was performed with respect to liposomes containing bSM (control condition).

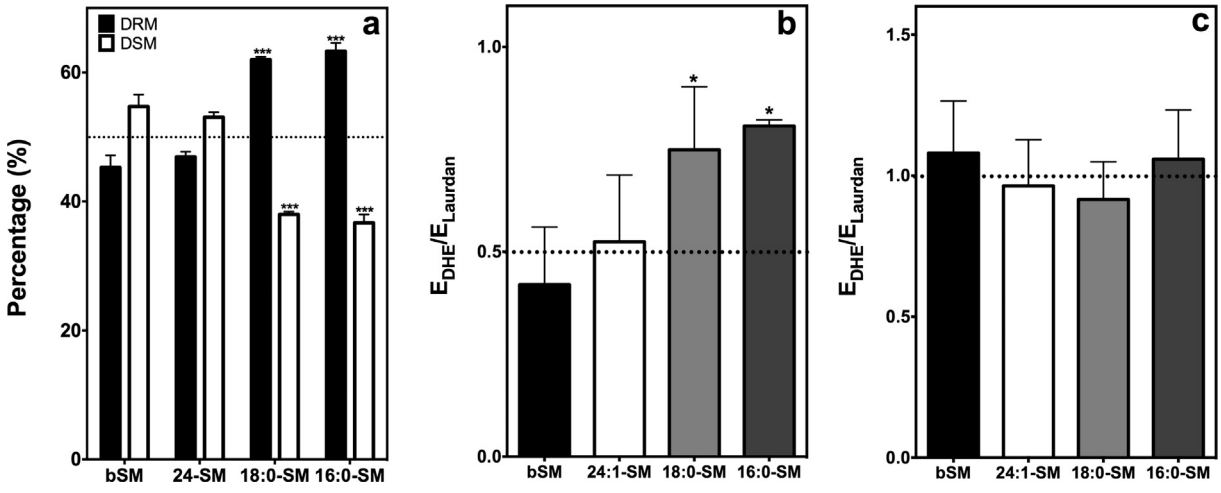

Fig. 4. AChR partition profile in membrane domains of POPC:Chol:SM (1:1:1) membranes with different SM species. (a) Percentage of [^{125}I]α-BTX binding to AChR in each fraction: DRM and DSM (black and white bar, respectively). (b) and (c) Förster resonance energy transfer efficiency (E) ratio between the AChR intrinsic fluorescence and the fluorescent probes DHE (E_{DHE}) and Laurdan ($E_{Laurdan}$) at 4 °C and 42 °C, respectively. Each column corresponds to the average ± SD of at least three different experiments. The comparison was performed with respect to liposomes containing bSM (control condition).

intensity. These domains showed also different biophysical properties, such as lipid order. The higher degree of order was observed with 18:0-SM, followed by 16:0-SM (Fig. 2). In the case of bSM, considerably richer in 18:0-SM than 24:1-SM, a behavior more similar to that of 24:1 was observed.

Differences in size, amount and/or lipid order of the Lo domains showed a direct correlation with the tendency of the AChR to localize in Lo domains (Fig. 4). A clear change in the AChR distribution between DRM and DSM fractions was evidenced mainly when bSM was replaced by 16:0-SM or by 18:0-SM, with an

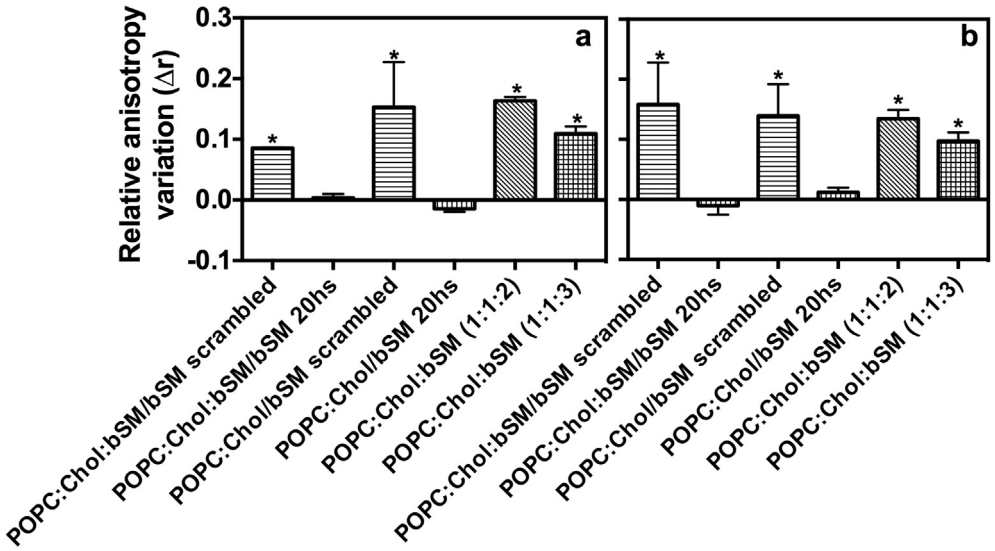

Fig. 5. Transbilayer asymmetry induction evaluation by fluorescence anisotropy. Transbilayer asymmetry was generated by facing lipid-only symmetric liposomes with MßCD-bSM MLVs. Samples after transbilayer asymmetry induction were renamed by adding "/bSM" to indicate the addition of bSM to their external hemilayer (e.g. POPC:Chol:bSM turns into POPC:Chol:bSM/bSM after asymmetry induction). Relative differences in fluorescence anisotropy (Δr) measurements of the fluorescence probes (a) DPH and (b) TMA-DPH at 4 °C between liposomes obtained by asymmetric induction and measured right after the induction asymmetry and liposomes performed with different conditions: liposomes obtained by asymmetric induction maintained at 4 °C and measured 20 hs later (*POPC:Chol:bSM/bSM 20 hs* or *POPC:Chol/bSM 20 hs)*; liposomes obtained by asymmetric induction, scrambled, reconstituted into symmetrical vesicles and measured right after reconstitution (*POPC:Chol:bSM/bSM scrambled* or *POPC:Chol/bSM scrambled)*; and symmetrical liposomes richer in bSM (*POPC:Chol:bSM 1:1:2* or *POPC:Chol:bSM 1:1:3)*. Each sample was divided in two and each one incubated at least 5 min with the corresponding fluorescent probe before taking the measurements. Each column corresponds to the average ± SD of at least three different experiments. All ternary liposomes were compared to POPC:Chol:bSM/bSM and all binary liposomes were compared to POPC:Chol/bSM.

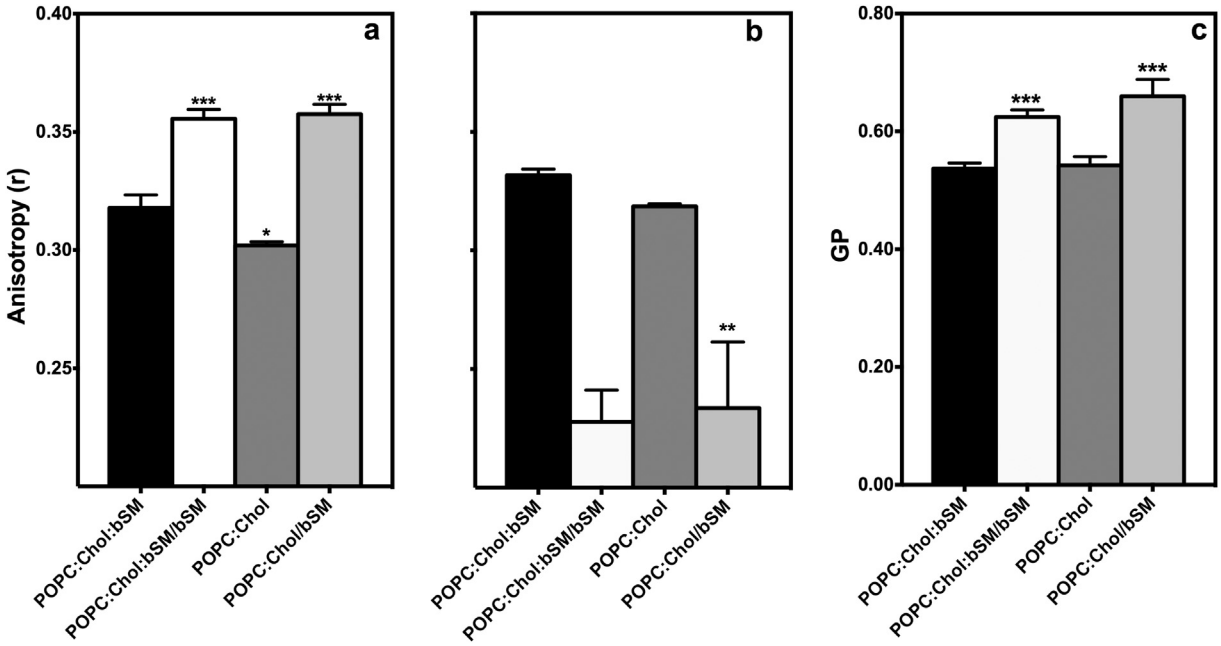

Fig. 6. Membrane order modification by transbilayer asymmetry induction. Transbilayer asymmetry was generated by facing AChR containing symmetric liposomes with MßCD-bSM MLVs. Fluorescence anisotropy (r) measurements of the fluorescence probes (a) DPH and (b) TMA-DPH and (c) Generalized Polarization (GP) of the fluorescence probe Laurdan at 4 °C of liposomes of AChR reconstituted in the symmetric liposomes POPC:SM:Chol (1:1:1) and POPC:Chol (1:1) and in the induced-transbilayer asymmetric liposomes POPC:SM:Chol/bSM and POPC:Chol/bSM membranes. Each column corresponds to the average ± SD of at least three different experiments. Each asymmetric condition were compared to their corresponding symmetric conditions (POPC:Chol:bSM or POPC:Chol).

increased occurrence of the AChR in DRMs. Reinforcing the fact that fractions obtained with 24:1-SM showed a behavior similar to that obtained with bSM, the replacement of bSM by 24:1-SM did not cause changes in the AChR preference for these fractions. Thus, although almost all SMs form Lo domains, each one confers particular properties to the domain, which have in turn a noticeable effect over the distribution of the AChR. SM with shorter and saturated acyl chains, like 16:0-SM and 18:0-SM, which have higher affinity for Chol [44], play an important role in the preferential distribution of the AChR protein in DRM. Unsaturated SM with

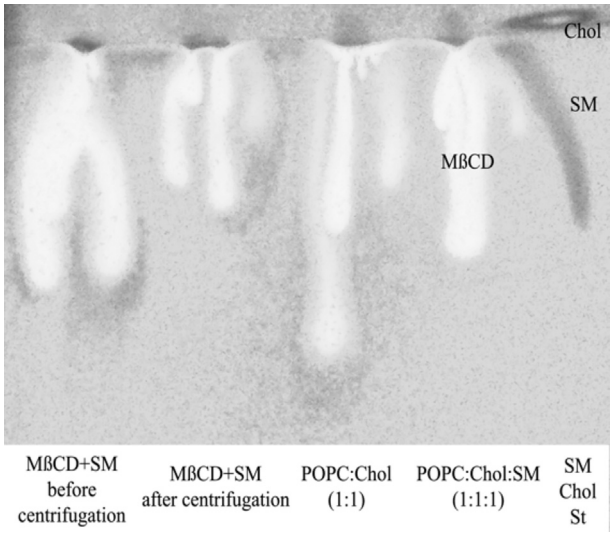

Fig. 7. Thin layer chromatography (TLC) of lipid extracts from supernatant of different asymmetry conditions. The amount of SM and Chol was qualitatively compared between the obtained supernatant from the following conditions from the left: the first and second lanes correspond to MβCD + SM mixture without contact with samples before and after the required centrifugation steps (controls of the total amount of SM and of the possible SM loss during the centrifugation steps, respectively); the third and fourth lanes correspond to MβCD after contact with either POPC:Chol (1:1) or POPC:Chol:bSM (1:1:1) membranes (controls of the remaining SM loaded to MβCD and of the possible Chol extraction by MβCD); and the fifth lane corresponds to Chol and SM standards.

longer chains, like 24:1-SM, lead to lack of preference of the AChR for either domain. It is also interesting to note that even though bSM is considerably richer in 18:0-SM than in 24:1-SM, the effect that the presence of 24:1-SM in the membrane has on AChR localization in Lo domains predominates over that exerted by 18:0-SM. To our knowledge, this is the first time that a transmembrane protein changes its preference for a certain membrane domain by changing just one lipid species that alters Lo domain properties. Furthermore, these results suggest that the type of SM present in the Lo domain is involved in the recruitment of AChR into *raft*-domains in native membranes.

Considering that natural membranes have transbilayer asymmetry and that raft-domains are postulated to be located mainly in the external hemilayer [58], we analyzed AChR distribution in transbilayer asymmetric LUVs highly enriched in SM in the external hemilayer. The excess of SM resulted in an increase of the amount of external domains with a higher lipid ordered (Fig. 6). AChR was found to have a higher preference to locate in these DRM fractions (Fig. 8). Again, a change in the properties/location of the Lo domains impacts on the AChR preference for this fraction. Whether this effect can be attributed to the transbilayer asymmetry or to the presence of domains with higher order needs further investigation. However, it is clear that exogenous lipids influence the localization of the AChR in the membrane. Similar results were recently published by Hussain et al. [63] demonstrating the importance of membrane asymmetry on integrin sequestering in raft-mimicking lipid mixtures. They showed that in symmetric bilayers $\alpha_v\beta_3$ receptors have a preference for Ld regions, whereas in asymmetric bilayer systems, they prefer Lo regions. Interestingly, the addition of native ligands mediated $\alpha_v\beta_3$ net translocation from Ld to Lo regions in symmetric bilayers without changing their preference for Lo domains in asymmetric models. The authors interpreted this observation on the basis of ligand-induced conformational changes, postulating two potential mechanisms of integrin sequestration: changes in hydrophobic matching and/or in integrin-lipid interactions [63].

Natural membranes are complex entities, with marked asymmetries and a large variety of lipids and proteins. They are the place where a huge amount of signals occur; and without any doubt, they participate in a great variety of these signaling processes [64].

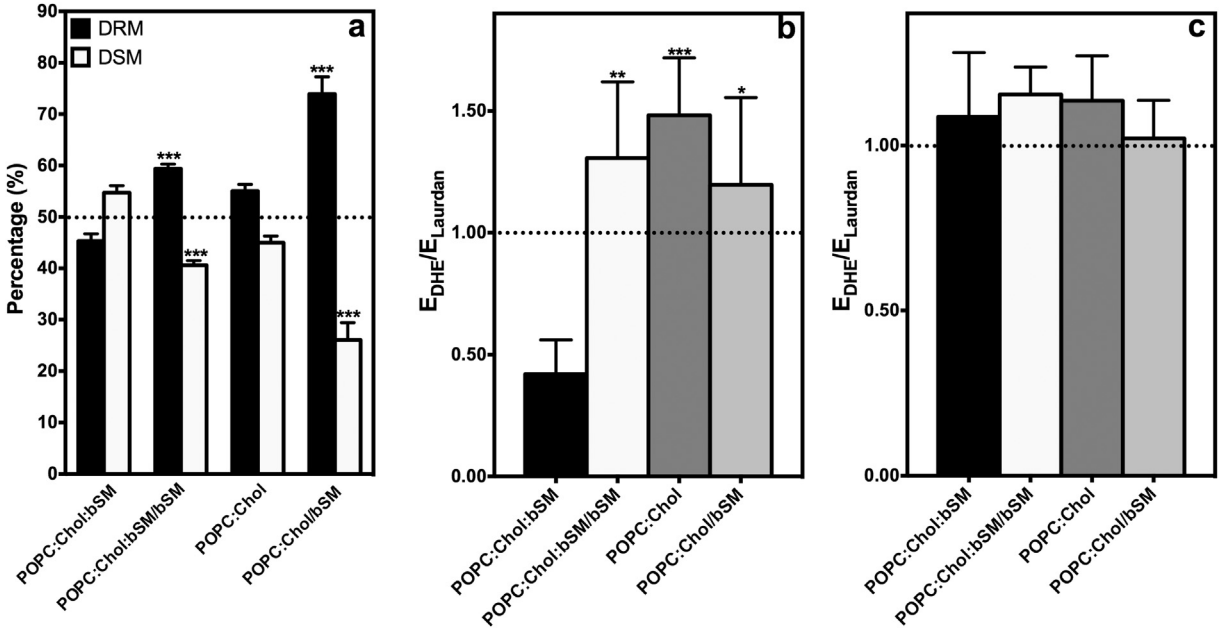

Fig. 8. AChR partition profile membrane domains obtained before and after induced transbilayer asymmetry. Transbilayer asymmetry was generated by facing AChR containing symmetric liposomes with MßCD-bSM MLVs. (a) Percentage of [^{125}I]α-BTX binding to AChR in each fraction (before and after induced transbilayer asymmetry): DRM and DSM (black and white bar, respectively). (b) and (c) Förster resonance energy transfer efficiency (E) ratio between the AChR intrinsic fluorescence and the fluorescent probes DHE (E_{DHE}) and Laurdan ($E_{Laurdan}$) at 4 °C and 42 °C, respectively. Each column corresponds to the average ± SD of at least three different experiments. The comparison was performed with respect to symmetric liposomes containing POPC.Chol:bSM.

Traditionally, the cell surface was described by the *fluid mosaic model* which posits the membrane as a two dimensional equilibrated fluid where lipids are mixed in a homogenous phase. Recent membrane models give a more complex picture of cell membrane organization. As explained by Rao and Mayor [18], assemblies of specific lipid and protein components at long/short spatial and temporal scales result in some level of compositional heterogeneity. One of these models is the *raft model* which initially postulated that Chol and sphingolipids spontaneously associate to form platforms where certain proteins can segregate. A role in building signaling complexes by membrane protein sorting is assigned to these segregated domains [20].

AChRs occur in clusters at the postsynaptic membrane [8]. In some instances it has been postulated that AChR clusters concentrate in raft-domains [9]. However, we reported that although the AChR has the potential to be in these domains, the complete protein shows no preference/rejection for Lo domains [23]. Additional, external signals must direct the protein to specific domains in the membrane. Here it is shown that SM composition plays an important role in determining the tendency of the AChR to partition in a given domain in model lipid systems. It is logical to suggest that in the natural membrane, the existence of different SM species could play a role in defining the localization of the AChR in ordered domains. The second factor identified here is transbilayer asymmetry. Introducing membrane asymmetry in an inherently symmetric model system resulted in AChR partitioning in Lo domains. It is thus clear from the present study that the AChR can localize in ordered lipid domains. This results from not only the protein's preference for a given membrane domain but from a variety of other factors, including the type of SM species in the ordered domain and the occurrence of transbilayer membrane asymmetry.

Acknowledgments

Many thanks are due to Dr. M. I. Aveldaño for the use of her laboratory facilities in part of the work. This work was supported by grants PIP 112-201101-00239 from the National Scientific and Technical Research Council of Argentina (CONICET); PGI 24/B168 from the Universidad Nacional del Sur and PICT 2012-2746 from the Ministry of Science, Technology and Innovative production (MINCYT) to S.S.A., and PIP 112-201101-01023 from CONICET and PICT 2011-0604 from MINCYT to F.J.B.

Appendix A. Supplementary data

Supplementary data related to this article can be found at http://dx.doi.org/10.1016/j.abb.2015.12.003.

References

[1] M.O. Ortells, G.G. Lunt, Evolutionary history of the ligand-gated ion-channel superfamily of receptors, Trends Neurosci. 18 (1995) 121–127.
[2] M. Mishina, T. Takai, K. Imoto, M. Noda, T. Takahashi, S. Numa, et al., Molecular distinction between fetal and adult forms of muscle acetylcholine receptor, Nature 321 (1986) 406–411.
[3] A. Karlin, Emerging structure of the nicotinic acetylcholine receptors, Nat. Rev. Neurosci. 3 (2002) 102–114.
[4] F.J. Barrantes, Structural basis for lipid modulation of nicotinic acetylcholine receptor function, Brain Res. Brain Res. Reviews 47 (2004) 71–95.
[5] F.J. Barrantes, Phylogenetic conservation of protein–lipid motifs in pentameric ligand-gated ion channels, Biochim. Biophys. Acta (BBA) – Biomem 1848 (9) (2015) 1796–1805.
[6] J.R. Sanes, J.W. Lichtman, Development of the vertebrate neuromuscular junction, Ann. Rev. Neurosci. 22 (1999) 389–442.
[7] A.G. Engel, The neuromuscular junction, Handb. Clin. Neurol. 91 (2008) 103–148.
[8] J.R. Sanes, J.W. Lichtman, Induction, assembly, maturation and maintenance of a postsynaptic apparatus, Nat. Rev. Neurosci. 2 (2001) 791–805.
[9] D. Zhu, W.C. Xiong, L. Mei, Lipid rafts serve as a signaling platform for nicotinic acetylcholine receptor clustering, J. Neurosci. 26 (2006) 4841–4851.
[10] J.A. Campagna, J. Fallon, Lipid rafts are involved in C95 (4, 8) agrin fragment-induced acetylcholine receptor clustering, Neuroscience 138 (1) (2006) 123–132.
[11] C.A. Báez-Pagán, Y. Martínez-Ortiz, J.D. Otero-Cruz, I.K. Salgado-Villanueva, G. Velázquez, A. Ortiz-Acevedo, et al., Potential role of caveolin-1-positive domains in the regulation of the acetylcholine receptor's activatable pool, Channels 2 (3) (2008) 180–190.
[12] J.O. Colón-Sáez, J.L. Yakel, The α7 nicotinic acetylcholine receptor function in hippocampal neurons is regulated by the lipid composition of the plasma membrane, J. Physiol. 589 (Pt.13) (2011) 3163–3174.
[13] G.M. Khan, M. Tong, M. Jhun, K. Arora, R.A. Nichols, beta-Amyloid activates presynaptic alpha7 nicotinic acetylcholine receptors reconstituted into a model nerve cell system: involvement of lipid rafts, Eur. J. Neurosci. 31 (5) (2010) 788–796.
[14] J.L. Brusés, N. Chauvet, U. Rutishauser, Membrane lipid rafts are necessary for the maintenance of the α7 nicotinic acetylcholine receptor in somatic spines of ciliary neurons, J. Neurosci. 21 (2) (2001) 504–512.
[15] F. Stetzkowski-Marden, K. Gaus, M. Recouvreur, A. Cartaud, J. Cartaud, Agrin elicits membrane lipid condensation at sites of acetylcholine receptor clusters in C2C12 myotubes, J. Lipid Res. 47 (2006) 2121–2133.
[16] R. Willmann, S. Pun, L. Stallmach, G. Sadasivam, A. Ferrao Santos, P. Caroni, C. Fuhrer, Cholesterol and lipid microdomains stabilize the postsynapse at the neuromuscular junction, EMBO J. 25 (17) (2006) 4050–4060.
[17] L.J. Pike, Rafts defined: a report on the keystone symposium on lipid rafts and cell function, J. Lipid Res. 47 (2006) 1597–1598.
[18] M. Rao, S. Mayor, Active organization of membrane constituents in living cells, Curr. Op. Cell Biol. 29 (2014) 126–132.
[19] K. Gowrishankar, S. Ghosh, S. Saha, C. Rumamol, S. Mayor, M. Rao, Active remodeling of cortical actin regulates spatiotemporal organization of cell surface molecules, Cell 149 (6) (2012) 1353–1367.
[20] F.J. Barrantes, Cell-surface translational dynamics of nicotinic acetylcholine receptors, Front. Synaptic Neurosci. 6 (art. 25) (2014) 1–16.
[21] S. Marchand, A. Devillers-Thièry, S. Pons, J.-P. Changeux, J. Cartaud, Rapsyn escorts the nicotinic acetylcholine receptor along the exocytic pathway via association with lipid rafts, J. Neurosci. 22 (2002) 8891–8901.
[22] R.F.M. de Almeida, L. Loura, M. Prieto, A. Watts, A. Fedorov, F.J. Barrantes, Cholesterol modulates the organization of the γ M4 transmembrane domain of the muscle nicotinic acetylcholine receptor, Biophys. J. 86 (2004) 2261–2272.
[23] V. Bermúdez, S.S. Antollini, G.A. Fernández-Nievas, M.I. Aveldaño, F.J. Barrantes, Partition profile of the nicotinic acetylcholine receptor in lipid domains upon reconstitution, J. Lipid Res. 51 (2010) 2629–2641.
[24] A.J. Crossthwaite, T. Seebacher, N. Masada, A. Ciruela, K. Dufraux, J.E. Schultz, et al., The cytosolic domains of Ca2+-sensitive adenylyl cyclases dictate their targeting to plasma membrane lipid raft, J. Biol. Chem. 280 (2005) 6380–6391.
[25] M. Yamabhai, R.G.W. Anderson, Second cysteine-rich region of EGFR contains targeting information for caveolae/rafts, J. Biol. Chem. 277 (2002) 24843–24846.
[26] P. Scheiffele, M.G. Roth, K. Simons, Interaction of influenza virus haemagglutinin with sphingolipid-cholesterol membrane domains via its transmembrane domain, EMBO J. 16 (1997) 5501–5508.
[27] J.E. Smotrys, M.E. Linder, Palmitoylation of intracellular signaling proteins. Regulation and function, Ann. Rev. Biochem. 73 (2004) 559–587.
[28] D.A. Zacharias, J.D. Violin, A.C. Newton, R.Y. Tsien, Partitioning of lipid-modified monomeric GFPs into membrane microdomains of live cells, Science 296 (2002) 913–916.
[29] L.J. Pike, The challenge of lipid rafts, J. Lipid Res. 50 (2009) S323–S328.
[30] E.G. Bligh, W.J. Dyer, A rapid method of total lipid extraction and purification, Can. J. Biochem. Physiol. 37 (1959) 911–917.
[31] D.A. Peñalva, N.E. Furland, G.H. Lopez, M.I. Aveldaño, S.S. Antollini, Unique thermal behavior of sphingomyelin species with nonhydroxy and 2-hydroxy very-long-chain (C28-C32) polyunsaturated fatty acids, J. Lipid. Res. 54 (2013) 2225–2235.
[32] C.J.B. daCosta, A.A. Ogrel, E.A. McCardy, M.P. Blanton, J.E. Baenziger, Lipid-protein interactions at the nicotinic acetylcholine receptor: a unique coupling between nicotinic receptors and phosphatidic acid containing lipid bilayers, J. Biol. Chem. 277 (2001) 201–208.
[33] O.H. Lowry, N.J. Rosebrough, L.A. Farr, R.J. Randall, Protein measurement with the Folin phenol reagent, J. Biol. Chem. 193 (1951) 265–275.
[34] P.R. Hartig, M.A. Raftery, Preparation of right-side-out, acetylcholine receptor enriched intact vesicles from *Torpedo californica* electroplaque membranes, Biochemistry 18 (7) (1979) 1146–1150.
[35] C. Gutierrez-Merino, I.C. Bonini de Romanelli, L.I. Pietrasanta, F.J. Barrantes, Preferential distribution of the fluorescent phospholipid probes NBD-phosphatidylcholine and Rhodamine-phosphatidylethanolamine in the exofacial leaflet of acetylcholine receptor-rich membranes from *Torpedo marmorata*, Biochemistry 34 (14) (1995) 4846–4855.
[36] H.-T. Cheng, Megha, E. London, Preparation and properties of asymmetric vesicles that mimic cell membranes effect upon lipid raft formation and transmembrane helix orientation, J. Biol. Chem. 284 (2009) 6079–6092.
[37] M.D. Abrámoff, P.J. Magalhães, S.J. Ram, Image processing with ImageJ, Biophot. Int. 11 (2004) 36–42.
[38] G. Rouser, S. Fkeischer, A. Yamamoto, Two dimensional thin layer

chromatographic separation of polar lipids and determination of phospholipids by phosphorus analysis of spots, Lipids 5 (1970) 494–496.
[39] T. Förster, Intermolecular energy migration and fluorescence, Ann. Phys. Leipz. 2 (1948) 55–75.
[40] S.S. Antollini, F.J. Barrantes, Disclosure of discrete sites for phospholipid and sterols at the protein–lipid interface in native acetylcholine receptor-rich membrane, Biochemistry 37 (47) (1998) 16653–16662.
[41] T. Parasassi, G. De Stasio, G. Ravagnan, R.M. Rusch, E. Gratton, Quantitation of lipid phases in phospholipid vesicles by the generalized polarization of Laurdan fluorescence, Biophys. J. 60 (1991) 179–189.
[42] V.L. Perillo, G.A. Fernández-Nievas, A.S. Vallés, F.J. Barrantes, S.S. Antollini, The position of the double bond in monounsaturated free fatty acids is essential for the inhibition of the nicotinic acetylcholine receptor, Biochim. Biophys. Acta – Biomem 1818 (2012) 2511–2520.
[43] M. Shinitzky, Y. Yuli, Lipid fluidity at the submacroscopic level: determination by fluorescence polarization, Chem. Phys. Lipids 30 (1982) 261–282.
[44] S. Jaikishan, J.P. Slotte, Effect of hydrophobic mismatch and interdigitation on sterol/sphingomyelin interaction in ternary bilayer membranes, Biochim. Biophys. Acta 1808 (2011) 1940–1945.
[45] R.F.M. de Almeida, A. Fedorov, M. Prieto, Sphingomyelin/phosphatidylcholine/cholesterol phase diagram: boundaries and composition of lipid rafts, Biophys. J. 85 (2003) 2406–2416.
[46] D. Lichtenberg, F. Goñi, H. Heerklotz, Detergent-resistant membranes should not be identified with membrane rafts, Trends biochem. Sci. 30 (2005) 430–436.
[47] S.L. Veatch, S.L. Keller, Organization in lipid membranes containing cholesterol, Phys. Rev. Lett. 89 (2002) 268101.
[48] S.L. Veatch, S.L. Keller, Separation of liquid phases in giant vesicles of ternary mixtures of phospholipids and cholesterol, Biophys. J. 85 (5) (2003) 3074–3083.
[49] O. Garvik, P. Benediktson, A.C. Simonsen, J.H. Ipsen, D. Wüstner, The fluorescent cholesterol analog dehydroergosterol induces liquid-ordered domains in model membranes, Chem. Phys. Lipids 159 (2009) 114–118.
[50] C. Dietrich, L.A. Bagatolli, Z.N. Volovyk, N.L. Thompson, M. Levi, K. Jacobson, et al., Lipid rafts reconstituted in model membranes, Biophys. J. 80 (2001) 1417–1428.
[51] L.A. Bagatolli, To see or not to see: lateral organization of biological membranes and fluorescence microscopy, Biochim. Biophys. Acta - Biomem 1758 (10) (2006) 1541–1556.
[52] L. Rajendran, K. Simons, Lipid rafts and membrane dynamics, J. Cell Sci. 118 (2005) 1099–1102.
[53] R.D. Kaiser, E. London, Location of diphenylhexatriene (DPH) and its derivatives within membranes: comparison of different fluorescence quenching analyses of membrane depth, Biochemistry 37 (1998) 8180–8190.
[54] M.P. Beseničar, A. Bavdek, A. Kladnik, P. Maček, G. Anderluh, Kinetics of cholesterol extraction from lipid membranes by methyl-β-cyclodextrin—A surface plasmon resonance approach, Biochim. Biophys. Acta 1778 (2008) 175–184.
[55] A. Choubey, R.K. Kalia, N. Malmstadt, A. Nakano, P. Vashishta, Cholesterol translocation in a phospholipid membrane, Biophys. J. 104 (11) (2013) 2429–2436.
[56] Q. Lin, E. London, Ordered raft domains induced by outer leaflet sphingomyelin in cholesterol-rich asymmetric vesicles, Biophys. J. 108 (9) (2015) 2212–2222.
[57] J. Bai, R.E. Pagano, Measurement of spontaneous transfer and transbilayer movement of bodipy-labeled lipids in lipid vesicles, Biochemistry 36 (1997) 8840–8848.
[58] P.F. Devaux, R. Morris, Transmembrane asymmetry and lateral domains in biological membranes, Traffic 5 (2004) 241–246.
[59] D. Marsh, L.I. Horvath, Structure, dynamics and composition of the lipid–protein interface. Perspectives from spin-labelling, Biochim. Biophys. Acta 1376 (1998) 267–296.
[60] I.C. Bonini, S.S. Antollini, C. Gutiérrez-Merino, F.J. Barrantes, Sphingomyelin composition and physical asymmetries in native acetylcholine receptor-rich membranes, Eur. Biophys. J. 31 (6) (2002) 417–427.
[61] Y. Barenholz, T.E. Thompson, Sphingomyelins in bilayers and biological membranes, Biochim. Biophys. Acta – Biomem 604 (1980) 129–158.
[62] P. Niemelä, M.T. Hyvönen, I. Vattulainen, Structure and dynamics of sphingomyelin bilayer: insight gained through systematic comparison to phosphatidylcholine, Biophys. J. 87 (2004) 2976–2989.
[63] N.F. Hussain, A.P. Siegel, Y. Ge, R. Jordan, C.A. Naumann, Bilayer asymmetry influences integrin sequestering in raft-mimicking lipid mixtures, Biophys. J. 104 (10) (2013) 2212–2221.
[64] D. Lingwood, K. Simons, Lipid rafts as a membrane-organizing principle, Science 327 (2010) 46–50.